# Role of C in $MgC_xNi_3$ investigated from first principles

P. Jiji Thomas Joseph and Prabhakar P. Singh
*Department of Physics, Indian Institute of Technology—Bombay, Mumbai 400076, India*
(Received 26 April 2005; published 23 August 2005)

The influence of vacancies in the C sublattice of $MgCNi_3$, on its structural, electronic, and magnetic properties are studied by means of the density-functional-based Korringa-Kohn-Rostoker Green's function method formulated in the atomic sphere approximation. Disorder is taken into account by means of coherent-potential approximation. Characterizations representing the change in the lattice properties include the variation in the equilibrium lattice constants, bulk modulus, and pressure derivative of the bulk modulus, and those of the electronic structure include the changes in the total, partial, and **k**-resolved density of states. The incipient magnetic properties are studied by means of the fixed-spin moment method of alloy theory, together in conjunction with the phenomenological Ginzburg-Landau equation for magnetic phase transition. The first-principles calculations reveal that due to the breaking of the C-Ni bonds, some of the Ni 3*d* states, which were lowered in energy due to strong hybridization, are transferred back to higher energies thereby increasing the itinerant character in the material. The Bloch spectral densities evaluated at the high symmetry points, however, reveal that the charge redistribution is not uniform over the cubic Brillouin zone, as new states are seen to be created at the Γ point, while a shift in the states on the energy scale are seen at other high symmetry points.

DOI: 10.1103/PhysRevB.72.064519 PACS number(s): 74.25.Jb, 71.20.Be, 71.15.Nc

## I. INTRODUCTION

Characterizations revealing the nature of pairing mechanism of the 8 K perovskite superconductor $MgCNi_3$ (Ref. 1) are at odds. The nuclear spin-lattice relaxation rate displays the typical behavior of isotropic *s*-wave superconductivity with a coherence peak below the transition temperature $T_C$.[2] However, the specific heat[1,3–6] and resistivity[1,5,7–9] measurements imply a moderately coupled superconductor,[5,6,10,11] which is well supported by the tunneling experiments[12] as well as theoretical calculations.[13,14] The penetration depth measurements, however, distinctly show a non-*s*-wave BCS feature at low temperature.[15] Hamiltonian-based model calculations suggest $MgCNi_3$ to be a *d*-wave superconductor.[16] A two-band model also has been proposed[3,4,17] to reconcile the controversies in the experiments. Hall coefficient and thermoelectric power data[5,7] show that the carriers are essentially electrons. However, it was also suggested that the holes in Ni 3*d* states could be responsible for the transport properties, in analogy with the holes in the O 2*p* states of perovskite oxide superconductors.[1] The constant scattering approximation also shows that the thermoelectric power is hole-like above 10 K.[18] In fact the multi-band model provides a consistent interpretation of the temperature dependence of the normal resistivity, Hall constant, and that of the thermoelectric power.[17]

The disparity in the experiments may arise due to the exactness in terms of stoichiometry. Compositions, namely $Mg_{1+z}C_xNi_3$ with $0.75 \leqslant z \leqslant 1.55$ and $0.50 \leqslant x \leqslant 1.55$, are reported,[19] when subjected to different synthesizing routes (for a review, see Ref. 20). The variation then suggests that the physical properties are intimately related to the temperature which can be thought to control the materials composition and/or configuration, making it sensitive to the chemical nature of the compound as well as the specific method used for crystal growth. For example, two different phases—the $\alpha$ and $\beta$—have been synthesized by changing the sintering temperature[19] with the $\beta$ phase being superconducting while the $\alpha$ phase remains nonsuperconducting. The major difference between these two phases is in the exact C content in the material. For high C content, the scanning experiments reveal the excess in terms of granules.[10] The change from grain boundary to core pinning by these intragranular nanoparticles near the superconducting transition temperature $T_C$ suggests that the arrangement of pinning sites in $MgCNi_3$ is quite unique.[10] However, the physical properties unveiled by the system are essentially a bulk property, not pertaining to any interfaces or microstructures. Nevertheless, the $T_C$ is sensitive to the C content which decreases with decreasing $x$ in $MgC_xNi_3$ and disappears for materials where $x \leqslant 0.9$.[21] The changes in the normal metal state properties of $MgC_xNi_3$ with respect to decreasing $x$ are what are emphasized in the present work.

The C in the octahedral interstitial site of $MgC_xNi_3$ has two major roles to play. The spatially extended C 2*p* orbitals strongly hybridize with the Ni 3*d*, thus delocalizing the electronic states. Delocalization leads to an overall reduction in its itinerant character, rendering a definite nonmagnetic state. Further, the presence of C expands the unit cell dimensions which favors soft Ni-derived phonon modes.[13] A recent C-isotope study[22] and B substitutions at C sites[23] show that in addition to the dominant Ni modes,[24,25] certain C modes are also important in the materials pairing mechanism.

According to the microscopic theory of superconductivity, the occurrence of vacancies may influence $T_c$ either through a modification in the value of the density of states at Fermi energy $N(E_F)$ or through modifying the electron-phonon coupling parameter, or both. The electron-phonon coupling parameter is proportional to $M\langle\omega^2\rangle$, where $M$ is the mass of the transition metal and $\langle\omega^2\rangle$ is the average squared moment of the phonon spectrum. One expects that vacancies in the C

 

sublattice of $MgC_xNi_3$ can have adverse effects on its lattice, electronic, and other related properties. It is shown in a previous report that the $N(E_F)$ decreases, rather abruptly, as an increasing function of vacancies.[26] The decrease may be attributed to the disorder smearing of the electronic bands, in particular to those which constitute the van Hove singularity-like feature just below the Fermi energy. However, it is possible that, if not at the Fermi energy, at least the upper valence band would get enriched in states due to breaking of the C-Ni bonds. This may happen because some of the Ni $3d$ states, which were lowered in energy due to strong hybridization, would be transferred back to the higher energies in proportion to the exact concentration of vacancies in the C sublattice. The redistribution can adversely affect the electronic-structure-related properties such as magnetism. Earlier, it was conjectured that since the hypothetical $MgNi_3$ shows a definite ferromagnetic ground state, the disappearance of superconductivity for $x \leqslant 0.9$ alloys would be intimately related to the pair-breaking effects.[27] This, however, is inconsistent with the experiments which detect no long-range magnetic ordering in $MgC_xNi_3$ alloys.[21,26]

First-principles density-functional-based calculations are carried out to study the changes in the equation of state parameters, viz. the equilibrium lattice constant, bulk modulus, and its pressure derivative as a function of $x$ in $MgC_xNi_3$. The changes in the electronic structure of the disordered $MgC_xNi_3$ as a function of $x$ are described by means of total and sublattice resolved partial density of states, calculated at their respective equilibrium lattice constants. On the other hand, the propensity of magnetism in $MgC_xNi_3$ with respect to $x$ is studied by means of the fixed spin moment method. The fit of the magnetic energy with magnetization to the Ginzburg-Landau functional, and the variation of the Ginzburg-Landau coefficients as a function of $x$ suggests that C deficiencies can enhance incipient magnetic properties. This is consistent with the self-consistent calculations which find a significant charge redistribution owing to the transfer of certain Ni $3d$ states, from the intermediate energies to that close to the Fermi energy.

## II. COMPUTATIONAL DETAILS

The ground state properties are calculated using the Korringa-Kohn-Rostoker (KKR) method[28] formulated in the atomic-sphere approximation (ASA) (Ref. 29 and references therein) with chemical disorder accounted by means of coherent-potential approximation (CPA).[30] For better refinements in the alloy energetics, the ASA is corrected by the use of both the muffin-tin correction for the Madelung energy[31] and the multi-pole moment correction to the Madelung potential and energy.[32,33] These corrections bring significant improvement in the accuracy by taking into consideration the nonspherical part of the polarization effects.[34] The partial waves in the KKR-ASA calculations are expanded up to $l_{\max}=3$ inside the atomic spheres. The multi-pole moments of the electron density have been determined up to $l^M_{\max}=6$ and then used for the multi-pole moment correction to the Madelung energy. The exchange-correlation effects are taken into consideration via the local density approximation (LDA) with Perdew and Wang parametrization.[35] The core states have been recalculated after each iteration. The calculations are partially scalar relativistic in the sense that although the wave functions are nonrelativistic, first-order perturbation corrections to the energy eigenvalues due to the Darwin and the mass-velocity terms are included. Further, screening constants $\alpha$ and $\beta$ were incorporated in the calculations, following the prescription of Ruban and Skriver.[32,33] These values were estimated from the order ($N$) locally self-consistent Green's function method[36] and were determined to be 0.83 and 1.18, respectively. The atomic sphere radii of Mg, C, and Ni were kept as 1.404, 0.747, and 0.849 of the Wigner-Seitz radius, respectively. The vacancies in the C sublattice are modeled with the help of empty spheres, and their radius is kept equal to that of C itself. The overlap volume of the atomic spheres was less than 15%, which is legitimate within the accuracy of the approximation.[37] The number of **k** points for determining the total energies were kept in excess—1771 **k** points in the irreducible wedge of the Brillouin zone. The convergence in charge density was achieved so that the root mean square of moments of the occupied partial density of states becomes smaller than $10^{-6}$. Numerical calculations of magnetic energy $\Delta E(M)$ for $MgC_xNi_3$ are carried out at their self-consistently determined equilibrium lattice constants using the fixed spin moment method.[38] In the fixed-spin moment method the total energy is obtained for given magnetization $M$, i.e., by fixing the numbers of electrons with up and down spins. In this case, the Fermi energies in the up and down spin bands are not equal to each other because the equilibrium condition would not be satisfied for arbitrary $M$. At the equilibrium $M$ two Fermi energies will coincide with each other. The total magnetic energy becomes minimum or maximum at this value of $M$.

## III. RESULTS AND DISCUSSION

### A. Equation of state

The estimation of the equilibrium lattice constant is a critical check to the various approximations involved in the method. The KKR-ASA-CPA method estimates the lattice constant of $MgCNi_3$ to be 7.139 a.u., which is $\sim 1\%$ less than the experimental value.[1] However, the value is consistent with an earlier full-potential based method.[18] This shows that with the muffin-tin correction[31] the energetics of the material is described more accurately, almost at par with the full-potential counterparts. In the neutral spheres approximation,[39] in which this correction is ignored, the equilibrium lattice constant for $MgCNi_3$ was determined to be 6.983 a.u.

Total energy minimization en route to the equilibrium lattice constants $a_{\mathrm{eq}}$ were extended to compositions studied in the range $0.8 \leqslant x \leqslant 1.0$ in $MgC_xNi_3$. To estimate the bulk modulus $B_{\mathrm{eq}}$ and its pressure derivative $B'_{\mathrm{eq}}$, one may use the third-order Birch-Murnaghan equation of state.[40,41] The variation of these equation of state parameters as a function of $x$ are shown in Fig. 1.

The structural parameters decrease as $x$ decreases in $MgC_xNi_3$. The rate of decrease in the equilibrium lattice constant with respect to $x$ is found to be consistent with

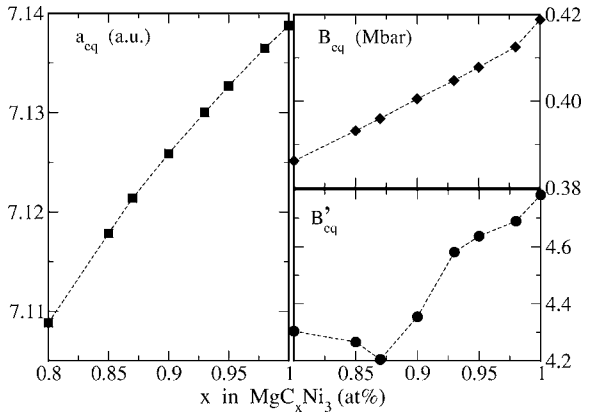


FIG. 1. The change in the equation of state parameters which include the equilibrium lattice constant ($a_{eq}$) in a.u., bulk modulus in Mbar, and the pressure derivative of the bulk modulus, as a function of $x$ in $MgC_xNi_3$ alloys.

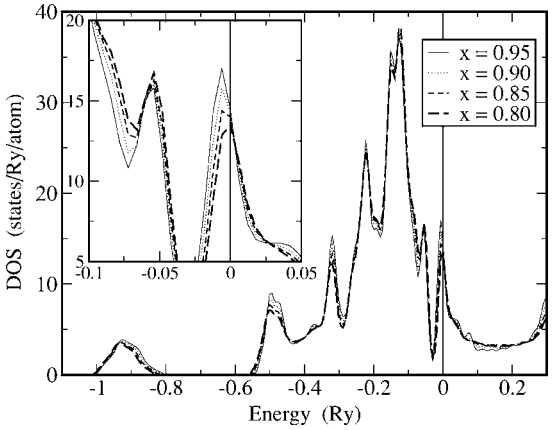


FIG. 2. The change in the total density of state as a function of $x$ in $MgC_xNi_3$ alloys. The inset refers to a blow up near the Fermi energy.

experiments.[21] The experiments find the rate of decrease as 0.187 a.u. (at % C)$^{-1}$, while the present calculations find it to be 0.179 a.u. (at % C)$^{-1}$. The decrease in $B_{eq}$ could be attributed to the fact that upon creation of vacancies the material becomes somewhat hollow, making it vulnerable to high compressibility. The change in $B'_{eq}$ as a function of $x$ shows a minimum in the range of $0.85<x<0.90$. The change in the slope of $B'_{eq}$ empirically suggests a change in the nature of chemical bonding as well as the lattice properties. In the Debye approximation for isotropic materials, which assumes a uniform dependence of the lattice frequencies with volume, one may express the average phonon frequency in terms of $B'_{eq}$ proportional to $(\delta \ln \omega)/(\delta \ln V_{eq})$, where $\omega$ is the average phonon frequency and $V_{eq}$ is the equilibrium volume of the unit cell. Note that $V_{eq}$ decreases with decrease in $x$, while $B'_{eq}$ decreases and then increases. Such a behavior indicates that the properties associated with the lattice could be different for $x<0.87$ and for $0.87<x<1.00$ alloys.

### B. Total and partial densities of states

Upon creation of vacancies in the C sublattice, some of the C 2*p*- Ni 3*d* bonds break and it can be expected that the 3*d* states may redistribute in the higher energy spectrum constituting the valence band. A possible way to examine this is to investigate the alloy density of states as a function of $x$ in $MgC_xNi_3$, which is shown in Fig. 2.

The present KKR-ASA-CPA calculations find $N(E_F)$ for $MgCNi_3$ to be 14.56 state/Ry-atom (or 5.35 states/eV-cell). The present value is in reasonable agreement with the previously reported values. For example, Szajek reports the value as 5.26 states/Ry-cell,[42] Mazin and Singh report as 4.99 states/Ry-cell,[18] Shim *et al.* as 5.34 states/Ry-cell,[14] and Rosner *et al.* as 4.8 states/Ry-cell.[43] Dugdale and Jarlborg[13] report $N(E_F)$ to be 6.35 and 3.49 states/eV-cell for two different band-structure methods with exchange-correlation effects considered in the LDA and using the experimental lattice constant. These results show that $N(E_F)$ is indeed sensitive to the type of electronic structure method employed and also to the numerical values of the parameters like that of the Wigner-Seitz radii and others. Note that these differences are significant as they control the proximity to magnetism in the Stoner model, as emphasized by Singh and Mazin.[18]

As a decreasing function of $x$, a rigid band description to account for the movement of $E_F$ fails for $MgC_xNi_3$. The peak characteristic of the Ni 3*d* bands which lie just below the Fermi energy, however, shows an insensitive change in its position on the energy scale. A similar feature has also been reported by Rosner *et al.*[43] for alkali metal substitutions at the Mg site in $MgCNi_3$. However, in $MgC_xNi_3$, due to disorder broadening of the bands, the $N(E_F)$ is found to decrease. The change in the total and sublattice resolved partial density of states at the Fermi energy is shown in Fig. 3. The initial change in $N(E_F)$ as $x$ decreases from 1.0 to 0.8 is gradual, however it displays a rapid change when C is reduced further. Such a decrease in $N(E_F)$ does not correspond to a rigid band picture. Moreover, the C 2*p* contribution to $E_F$ decreases monotonically at the rate of ~0.709 states/Ry-atom per at % of C, while Ni 3*d* contribution remains more or less unaffected for the range of alloys in $0.95<x<1.00$.

An earlier calculation based on CPA in the LMTO formalism finds a drastic linear decrease in $N(E_F)$ as a decreasing

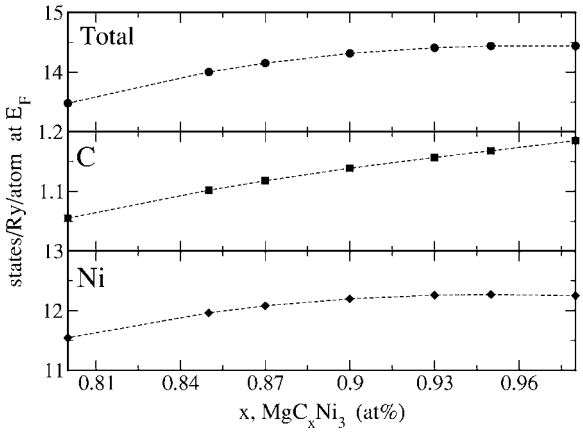


FIG. 3. The change in the total, C, and Ni contributions to the density of states at the Fermi energy as a function of $x$ in $MgC_xNi_3$ alloys.

function of $x$.[26] The authors report $N(E_F)$ to be 4.26 states/eV-cell ($\simeq$11.59 states/Ry-atom) at $x=0.977$ which decreases quite linearly to 3.14 states/eV-cell ($\simeq$8.54 states/Ry-atom) at $x=0.85$. The present calculations, however, observe a slightly different trend in the change of $N(E_F)$ with decreasing $x$ in $MgC_xNi_3$. The $N(E_F)$ at $x=0.98$ is calculated as 14.44 states/Ry-atom and that at $x=0.85$ to be 14.00 states/Ry-atom. The discrepancy may be due to the assumption of a particular lattice constant (experimental value) in the previous TB-LMTO-CPA calculations.[26]

As a prelude to understanding the overall shift in the bands as a function of $x$ in $MgC_xNi_3$, one may look at the shift in the potential parameters, in particular the bottom of the band ${}^BB$ and the center of the band ${}^BC$. The center of the Ni $3d$ band, ${}^BC_{\mathrm{Ni}}$ shifts approximately by +2.6 mRy from $x=1.0$ to 0.8 in $MgC_xNi_3$. Note that here +(−) represents the movement of the corresponding potential parameter towards (away) the Fermi energy. This is a clear revelation of the fact that the upper valence band becomes enriched with states, as $x$ is decreased in $MgC_xNi_3$. Note that due to hybridization with the C $2p$ states, some of the Ni $3d$ states in $MgCNi_3$ are lowered in energy. Upon creation of vacancies, a few of the $p$-$d$ bonds break and result in charge redistribution. We also observe that the ${}^BC_{\mathrm{Mg}}$ shifts away from the Fermi energy by −0.51 Ry from $x=1.0$ to 0.8. In fact, the $CNi_6$ octahedra is a covalently built complex to which the strong electropositive Mg is thought to have donated its outermost valence electrons. The crystal geometry suggests six Ni atoms as the first nearest neighbors to C with a bond length of 3.60 a.u., and eight Mg atoms as its second nearest neighbors with a bond distance of 6.25 a.u. in the unit cell. The Mg-Ni bond length is 5.09 a.u., and, as such for Mg's the first coordination shell is comprised of 12 Ni atoms. For Ni's the second nearest coordination shell carries four Mg atoms. Hence, the charge redistribution arising due to the breaking of the $p$-$d$ bonds is consistent with the fact that a larger fraction of the charge is transferred back to the Mg sublattice, in comparison with that of the Ni sublattice.

The shift in the ${}^BC_{\mathrm{Ni}}$ towards the Fermi energy indicates an accumulation of Ni $d$ states in the upper valence band which then opens up two possibilities for the disappearance of superconductivity: (*i*) The transfer of the states from low energy to higher energy states would increase the itinerant nature of electrons, thus enhancing the possibility of spin-fluctuations, and (*ii*) if the Ni $3d$ holes are responsible for superconducting pairing mechanism, then these states would be annihilated. To proceed further, one may require to decompose the density of the states along various high symmetry points and/or directions of the cubic Brillouin zone.

### C. Bloch spectral density of states

A convenient quantity to describe the **k**-resolved density of states of substitutionally disordered systems is the Bloch spectral function $A_B(\mathbf{k},E)$, which is the number of states per energy ($E$) and wavelength. In the case of pure metals the function is simply a sum of delta functions either as function of $E$ at a constant wave vector **k** or as a function of the wave vector **k** for a constant value of the energy. For constant $E$ $=E_F$, where $E_F$ is the Fermi energy the positions of the peaks in **k** space define the Fermi surface of the metal (see Refs. 29 and 44 and references therein). The **k**-space representation is a good description of the electronic structure of the alloy, although strictly speaking there is periodicity only on the average. In alloys, the Bloch spectral functions have their peaks lowered and broadened due to disorder. Thus, a Fermi surface for the alloy is still defined through the positions of the peaks but these peaks have a finite width.

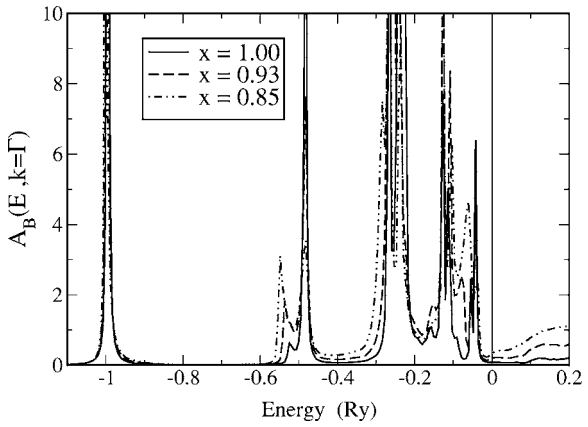


FIG. 4. The changes in the Bloch spectral density of states $A_B(\mathbf{k},E)$ in arbitrary units, resolved at $\mathbf{k}=\Gamma$ for $MgC_xNi_3$ alloys, using the LDA KKR-ASA-CPA method. The vertical line through the energy zero represents the Fermi energy.

The states at the $\Gamma$ point of the Brillouin zone are shown in Fig. 4. The states corresponding to −1 Ry are primarily composed of Mg $3s$ states. The C $2p$-Ni $3d$ hybrids form a complex in the energy range $-0.6<E<E_F$, where $E_F$ is taken as the zero of the energy scale. As a function of vacancy concentration, it is clear from Fig. 4 that a rigid-band picture is violated. States are redistributed at this high symmetry point, with a few of the Ni $3d$ states lifted to higher energies, particularly in the range $-0.1<E<E_F$. The peak corresponding to −0.5 Ry has in it a component of Mg $3s$ - Ni $3d$ hybrid, which as a function of $x$ lowers in energy. The sharp structure just below the Fermi energy is characteristic of Ni $3d$, which is less sensitive to the vacancy concentration. What follows from Fig. 4 is that the effects of vacancies are restricted to the energy range $-0.6<E<E_F$, with a significant redistribution of states, leading to an enhanced Ni $3d$ character at $E_F$. There is a slight increase in the density of states at $E_F$, which is far from any rigid-band interpretation.

A flat band running close to the $M$ point of the Brillouin zone has been mapped as a singularity in the DOS of $MgCNi_3$.[43] It has been emphasized that this singularity could induce magnetic instability upon 0.5 holes when introduced.[13,43] Figure 5 shows the changes in the Bloch spectral function for $MgC_xNi_3$ alloys at the $M$ point of the Brillouin zone. The states near the Fermi energy are primarily Ni $3d$ in character and do not show any significant change with increase in vacancies. The major effect of disorder is contained in two energy regions, concentrated at −0.5 and −0.2 Ry, respectively. These states result from a strong hybridization effect of Ni $3d$ and C $2p$ bands. Upon the creation of vacancies, the states concentrated around

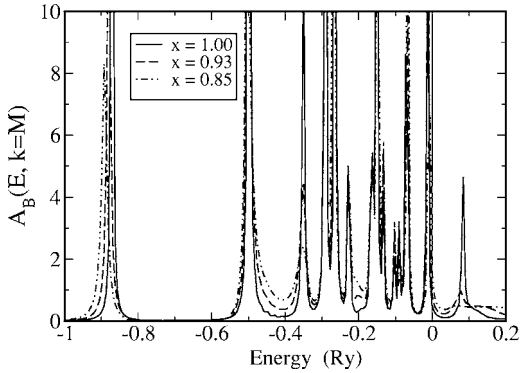


FIG. 5. The changes in the Bloch spectral density of states $A_B(\mathbf{k},E)$ in arbitrary units, resolved at $\mathbf{k}=M$ for $MgC_xNi_3$ alloys, using the LDA KKR-ASA-CPA method. The vertical line through the energy zero represents the Fermi energy.

−0.5 Ry are raised in energy. The peak at −0.4 Ry lowers in height, and the states are transferred to −0.2 Ry. The Fermi energy is almost pinned at the foot of the sharp singularity, thus maintaining the overall characteristic property of the alloy as a function of $x$ in $MgC_xNi_3$ alloys. The peak that evolves towards the bottom of the valence band is that of the Mg 3*s* band, which moves slightly towards lower energy. We note that in ASA formalism, the height of the spectral peak at a particular energy does not exactly refer to the states it holds, since the relevant matrix elements are ignored. However, a comparison may still be useful, since the approximations involved in the calculations are the same.

Figure 6 shows the redistribution of the states at the $R$ point of the Brillouin zone in $MgC_xNi_3$ as a function of $x$. The states residing deep in energy are due to the Mg 3*s* states, which move down as a function of increasing $x$. The major effects take place where C 2*p* bands are positioned, i.e., at around −0.45 and −0.18 Ry. The states in the energy range $-0.18<E<E_F$ are strictly Ni 3*d* in character, which is least affected.

The importance of the $X$ point lies in the hole states it accommodates, which is characterized by a peak just above the Fermi energy. (See Fig. 7.) As charge redistributes, with the upper valence band becoming more Ni 3*d* in character,

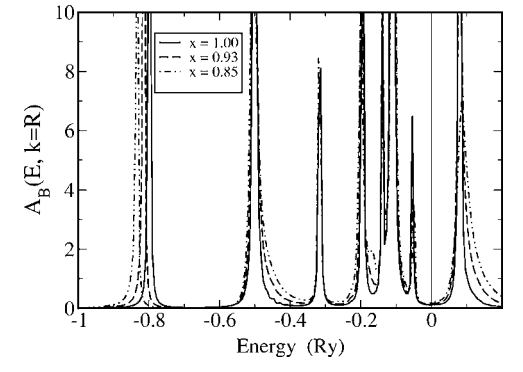


FIG. 6. The changes in the Bloch spectral density of states $A_B(\mathbf{k},E)$ in arbitrary units, resolved at $\mathbf{k}=R$ for $MgC_xNi_3$ alloys, using the LDA KKR-ASA-CPA method. The vertical line through the energy zero represents the Fermi energy.

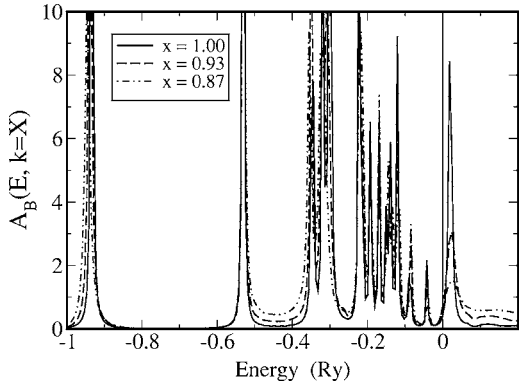


FIG. 7. The changes in the Bloch spectral density of states $A_B(\mathbf{k},E)$ in arbitrary units, resolved at $\mathbf{k}=X$ for $MgC_xNi_3$ alloys, using the LDA KKR-ASA-CPA method. The vertical line through the energy zero represents the Fermi energy.

the hole states are, however, not annihilated. Instead, the height of the peak decreases, showing a greater dispersion of the bands. However, as for other high symmetry points, one can see the distortion in those specific regions where C 2*p* states dominate.

In all cases, one finds that vacancies do not mimic a rigid band scenario. Some of the low-lying Ni 3*d* states, due to hybridization with C 2*p* states, are restored back to the higher energies when the bonds break. Charge transfer to the Mg sublattice is seen to occur via movement of the Mg 3*s* peaks to lower energies as well as an increase in the height of the peaks. As the charge redistributes, the nature of the bonding could be adversely affected. The covalent character of $MgC_xNi_3$ then may decrease as a decreasing function of $x$.

### D. Magnetic properties

Incipient magnetism, due to delocalization of the Ni 3*d* states owing to the strong hybridization with the C 2*p*, is probable in $MgCNi_3$. Following the Stoner criteria, it has been anticipated that spin fluctuations may coexist with superconductivity in $MgC_xNi_3$.[18] This, however, had been later confirmed in experiments.[2,45]

Self-consistent calculations, down to $x=0.8$ in $MgC_xNi_3$, do not find any magnetic solution. Both spin polarized and spin unpolarized show degeneracy in their total energies. To understand the change in the incipient magnetic properties, as a function of $x$ in $MgC_xNi_3$ alloys, one may then adopt the fixed-spin-moment method[38] by which the energy difference between a magnetic state with magnetic moment $M$ and the paramagnetic state, $\Delta E(M)[=E(M)-E(0)]$, for given values of $M$, can be calculated. The calculated $\Delta E(M)$ is then fitted to the Ginzburg-Landau equation of form $\Sigma_{n>0}(1/2n)a_{2n}M^{2n}$. The calculated results of $\Delta E(M)$ are shown in Fig. 8. The numbers shown in the figure denote the C concentration. It can be clearly seen that the curve of $\Delta E(M)$ is rather flat near $M=0$ and the flatness increases as $x$ decreases. The curve is fit to the form of a power series of $M^{2n}$ up to the term for $n=3$, for the polynomial as mentioned above. The variation of the coefficients, $a_2$ in units of $T/\mu_B$, $a_4$ in $T/\mu_B^3$, and $a_6$ in $T/\mu_B^5$ as a function of $x$, calculated at

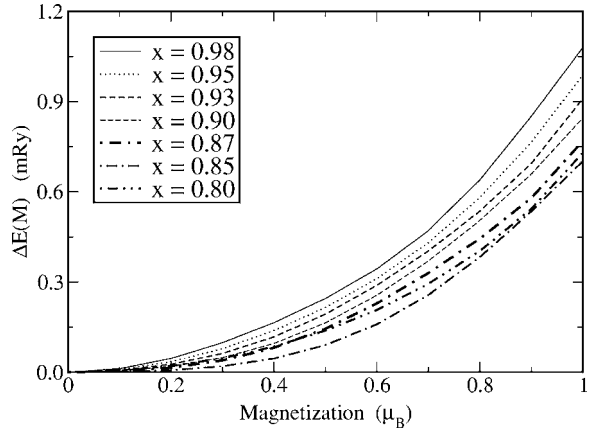


FIG. 8. The variation in the $\Delta E(M)$ in mRy as a function of $M$ expressed in Bohr magnetons of $MgC_xN$ alloys with $x$ as indicated in the legend box.

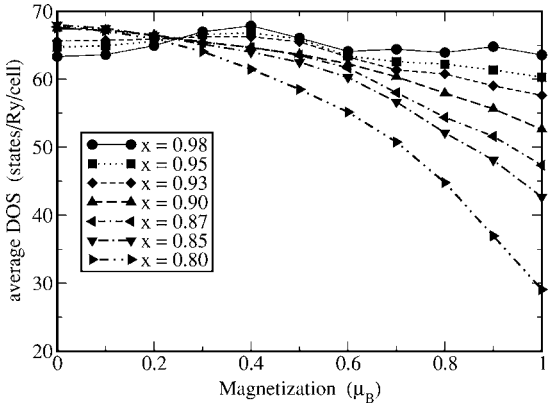


FIG. 10. The variation in the average DOS at $E_F$ as a function of magnetization for different $x$ in $MgC_xNi_3$ alloys from the LDA fixed spin calculations.

the respective equilibrium lattice constants, are shown in Fig. 9. The propensity of magnetism can be inferred from the sign of the coefficient which is quadratic in $M$, i.e., $a_2$. The coefficient $a_2$ is the measure of the curvature and is positive definite when the total energy minimum is at $M=0$. This refers to the paramagnetic case. When $a_2$ becomes negative, it infers that there exists a minimum in the $E$-$M$ curve other than $M=0$ which then points to a ferromagnetic phase. The higher order coefficients $a_4$ and $a_6$ are also significant and control the variation. In fact, $a_4$ determines whether for a system there exists a metastable state or not.

Consider a case where $a_2$ is small and positive while $a_4$ is relatively large and negative. In such a case, the calculations extended to large values of $M$ would tend to show a metastable state away from the total energy minimum. Often, calculations for large values of $M$, implying large applied external fields, can lead to ambiguous results. Hence, it is more accurate to carry out calculations for smaller values of $M$ and use the above-mentioned polynomial function up to the minimum order, where the curve fits with sufficient accuracy.

Figure 9 shows that for $x \rightarrow 0.87$, from the C-rich side, the alloys tend to enhance their latent magnetic properties. One

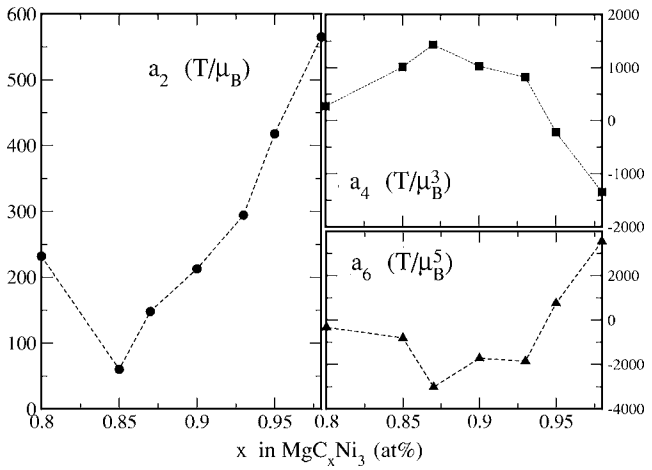


FIG. 9. The Ginzburg-Landau coefficients, $a_2$ expressed in $(T/\mu_B)$ and $a_2$ in $(T/\mu_B^3)$ for $MgC_xNi_3$ alloys as a function of $x$, from the LDA fixed spin calculations.

may also note that $a_4$ tends to become large and negative. This, however, is complemented by an opposite variation in the coefficient $a_6$. Hence, in the renormalized approach to include corrections due to spin-fluctuations like those given in Ref. 46, they would tend to cancel out, in proportion, preserving the trend in the variation of $a_2$. Thus, it becomes more or less conclusive within the approach that the incipient magnetic properties associated with C nonstoichiometry in $MgC_xNi_3$ would increase as a function of vacancies in the C sublattice. If one considers the proximity of $a_2 \rightarrow 0$ as an indication of spin fluctuations, then the calculations within the approximation clearly show that effects of spin fluctuations would be dominant in deciding the incipient magnetic properties of $MgC_xNi_3$ as a function of decreasing C. This is consistent with the movement of the center of the Ni $3d$ bands towards Fermi energy, as well as a very little change in the $N(E_F)$ as a function of decreasing $x$, determined in the self-consistent calculations. Since magnetism is controlled by $N(E_F)$, one may calculate the average density of states over the two spin bands in the fixed-spin moment method. The variation of this quantity as a function of $M$, for $x$ in $MgC_xNi_3$ alloys, is shown in Fig. 10. Note that lattice relaxation could be important[47] and particularly when $x$ increases in $MgC_xNi_3$. However, the results that are discussed are strictly for a case where one may find a rigid underlying lattice, and also that the vacancies spread in the alloy is random.

Thus, in general, it follows that as $x$ decreases in $MgC_xNi_3$, the propensity of magnetism increases. However, since $N(E_F)$ decreases, the stoner criteria is less fulfilled, making the material paramagnetic definite according to the itinerant models of magnetism.

## IV. SUMMARY AND CONCLUSIONS

The change in the equation of state parameters, density of states, and magnetic properties of $MgC_xNi_3$ are studied by means of the KKR-ASA-CPA method. Both lattice constant and bulk modulus decrease with decreasing $x$, while the pressure derivative of the bulk modulus, which is proportional to the average phonon frequency of the material in the Debye

approximation, is found to show an anomaly at about $x \sim 0.87$. The $N(E_F)$ decreases, however not as expected by a rigid band model. The Bloch spectral density evaluated at the $\Gamma$ point shows creation of new states below $E_F$ while for other high symmetry points they are shifted on the energy scale. The change in the coefficient $a_2$ in the Ginzburg-Landau equation for magnetic phase transition towards lower values suggests that incipient magnetic properties may be enhanced as a decreasing function of $x$ in $MgC_xNi_3$ alloys. This is consistent with the fact that due to bond breaking, some of the low lying Ni $3d$ states are transferred to higher energies, increasing the itinerancy of the material.

## ACKNOWLEDGMENTS

The authors would like to thank Hans L. Skriver and Andrei V. Ruban for their KKR-ASA-CPA code used in the present work. One of us (P.J.T.J.) would like to thank Andrei V. Ruban for discussion on the theory and implementation of code. Discussions with Dr. Igor I. Mazin on the various aspects of materials properties are gratefully acknowledged.

[1] T. He, K. A. Regan, M. A. Hayward, A. P. Ramirez, Y. Wang, P. Khalifah, T. He, J. S. Slusky, N. Rogado, K. Inumaru, M. K. Haas, H. W. Zandbergen, N. P. Ong, and R. J. Cava, Nature (London) **411**, 54 (2001).
[2] P. M. Singer, T. Imai, T. He, M. A. Hayward, and R. J. Cava, Phys. Rev. Lett. **87**, 257601 (2001).
[3] A. Walte, G. Fuchs, K.-H. Muller, A. Handstein, K. Nenkov, V. N. Narozhnyi, S.-L. Drechsler, S. Shulga, L. Schultz, and H. Rosner, Phys. Rev. B **70**, 174503 (2004).
[4] H. Rosner, M. D. Johannes, W. E. Pickett, G. Fuchs, A. Walte, S.-L. Drechsler, S. V. Shulga, K.-H. Muller, A. Handstein, K. Nenkov, J. Freudenberger, and L. Schultz, Physica C **388-389**, 563 (2003).
[5] J.-Y. Lin, P. L. Ho, H. L. Huang, P. H. Lin, Y.-L. Zhang, R.-C. Yu, C.-Q. Jin, and H. D. Yang, Phys. Rev. B **67**, 052501 (2003).
[6] M. S. Park, J. S. Giim, S. H. Park, Y. W. Lee, S. I. Lee, and E. Choi, Supercond. Sci. Technol. **17**, 274 (2004).
[7] S. Y. Li, R. Fan, X. H. Chen, C. H. Wang, W. Q. Mo, K. Q. Ruan, Y. M. Xiong, X. G. Luo, H. T. Zhang, L. Li, Z. Sun, and L. Z. Cao, Phys. Rev. B **64**, 132505 (2001).
[8] S. Y. Li, W. Q. Mo, M. Yu, W. H. Zheng, C. H. Wang, Y. M. Xiong, R. Fan, H. S. Yang, B. M. Wu, L. Z. Cao, and X. H. Chen, Phys. Rev. B **65**, 064534 (2002).
[9] T. G. Kumary, J. Janaki, A. Mani, S. M. Jaya, V. S. Sastry, Y. Hariharan, T. S. Radhakrishnan, and M. C. Valsakumar, Phys. Rev. B **66**, 064510 (2002).
[10] L. D. Cooley, X. Song, J. Jiang, D. C. Larbalestier, T. He, K. A. Regan, and R. J. Cava, Phys. Rev. B **65**, 214518 (2002).
[11] J-Y. Lin, P. H. Lin, P. L. Ho, H. L. Huang, Y-L. Zhang, R-C. Yu, C-Q. Jin, and H. D. Yang, J. Supercond. **15**, 485 (2002).
[12] L. Shan, H. J. Tao, H. Gao, Z. Z. Li, Z. A. Ren, G. C. Che, and H. H. Wen, Phys. Rev. B **68**, 144510 (2003).
[13] S. B. Dugdale and T. Jarlborg, Phys. Rev. B **64**, 100508(R) (2001).
[14] J. H. Shim, S. K. Kwon, and B. I. Min, Phys. Rev. B **64**, 180510(R) (2001).
[15] R. Prozorov, A. Snezhko, T. He, and R. J. Cava, Phys. Rev. B **68**, 180502(R) (2003).
[16] C. M. Granada, C. M. da Silva, and A. A. Gomes, Solid State Commun. **122**, 269 (2002).
[17] K. Voelker and M. Sigrist, cond-mat/0208367 (unpublished).
[18] D. J. Singh and I. I. Mazin, Phys. Rev. B **64**, 140507(R) (2001).
[19] A. Ren, G. C. Che, S. L. Jia, H. Chen, Y. M. Ni, G. D. Liu, and Z. X. Zhao, Physica C **371**, 1 (2002).
[20] S. Mollah J. Phys.: Condens. Matter **16**, R1237 (2004).
[21] T. G. Amos, Q. Huang, J. W. Lynn, T. He, and R. J. Cava, Solid State Commun. **121**, 73 (2002).
[22] T. Klimczuk, R. J. Cava, cond-mat/0410504 (unpublished).
[23] T. Klimczuk, M. Avdeev, J. D. Jorgensen, and R. J. Cava, cond-mat/0412551 (unpublished).
[24] A. Yu. Ignatov, S. Y. Savrasov, and T. A. Tyson, Phys. Rev. B **68**, 220504(R) (2003).
[25] R. Heid, B. Renker, H. Schober, P. Adelmann, D. Ernst, and K.-P. Bohnen, Phys. Rev. B **69**, 092511 (2004).
[26] L. Shan, K. Xia, Z. Y. Liu, H. H. Wen, Z. A. Ren, G. C. Che, and Z. X. Zhao, Phys. Rev. B **68**, 024523 (2003).
[27] I. R. Shein and A. L. Ivanovskii, J. Struct. Chem. **43**, 168 (2002)
[28] J. S. Faulkner, Prog. Mater. Sci. **27**, 1 (1982).
[29] I. Turek, V. Drchal, J. Kudrnovsky, M. Sob, and P. Weinberger, *Electronic Structure of Disordered Alloys, Surfaces and Interfaces* (Kluwer Academic Publishers, Dordrecht, 1997).
[30] P. Soven, Phys. Rev. **156**, 809 (1967).
[31] N. E. Christensen and S. Satpathy, Phys. Rev. Lett. **55**, 600 (1985).
[32] A. V. Ruban and H. L. Skriver, Phys. Rev. B **66**, 024201 (2002).
[33] A. V. Ruban, S. I. Simak, P. A. Korzhavyi, and H. L. Skriver Phys. Rev. B **66**, 024202 (2002).
[34] A. V. Ruban and H. L. Skriver, Comput. Mater. Sci. **15**, 119 (1999).
[35] J. P. Perdew and Y. Wang, Phys. Rev. B **45**, 13244 (1992).
[36] I. A. Abrikosov, S. I. Simak, B. Johansson, A. V. Ruban, and H. L. Skriver Phys. Rev. B **56**, 9319 (1997).
[37] Hans L. Skriver, *The LMTO method, Muffin Tin Orbitals and Electronic Structure* (Springer Verlag, New York, 1984).
[38] K Schwarz and P Mohn, J. Phys. F: Met. Phys. **14**, L129 (1984).
[39] P. P. Singh and A. Gonis, Phys. Rev. B **49**, 1642 (1994).
[40] F. Birch, J. Geophys. Res. **57**, 227 (1952).
[41] F. D. Murnaghan, *Finite Deformation of an Elastic Solid* (Wiley, New York, 1951).
[42] A. Szajek, J. Phys.: Condens. Matter **13**, L595 (2001).
[43] H. Rosner, R. Weht, M. D. Johannes, W. E. Pickett, and E. Tosatti, Phys. Rev. Lett. **88**, 027001 (2002).
[44] P. Weinberger, *Electron Scattering Theory for Ordered and Disordered Matter* (Oxford Sci. Publications, Oxford, 1990).
[45] G. Garbarino, M. Monteverde, M. Nunez-Regueiro, C. Acha , R. Weht, T. He, K. A. Regan, N. Rogado, M. Hayward, and R. J. Cava, Physica C **408-410**, 754 (2004).
[46] H. Yamada and K. Terao, Phys. Rev. B **59**, 9342 (1999).
[47] A. Yu. Ignatov, L. M. Dieng, T. A. Tyson, T. He, and R. J. Cava, Phys. Rev. B **67**, 064509 (2003).